Mon. Not. R. Astron. Soc. **262,** 151–163 (1993)

The modulation of radiation in an electron–positron plasma

R. T. Gangadhara,[1,2] V. Krishan[1] and P. K. Shukla[3]
[1]*Indian Institute of Astrophysics, Bangalore 560 034, India*
[2]*Joint Astronomy Programme, Department of Physics, Indian Institute of Science, Bangalore 560 012, India*
[3]*Institut für Theoretische Physik IV, Ruhr-Universität Bochum, D-4630 Bochum 1, Germany*

Accepted 1992 October 20. Received 1992 September 14; in original form 1992 March 27

ABSTRACT

The modulational instability of a large-amplitude, linearly polarized electromagnetic wave propagating in an electron–positron plasma is considered, including the combined effect of relativistic mass variation of the plasma particles, harmonic generation, and the non-resonant, finite-frequency electrostatic density perturbations, all caused by the large-amplitude radiation field. The radiation from many strong sources, such as AGN and pulsars, has been observed to vary over a host of time-scales. It is possible that the extremely rapid variations in the non-thermal continuum of AGN, as well as in the non-thermal radio radiation from pulsars, can be accounted for by the modulational instabilities to which radiation may be subjected during its propagation out of the emission region.

Key words: instabilities – plasmas – radiation mechanisms: miscellaneous – pulsars: general – quasars: general – radio continuum: galaxies.

1 INTRODUCTION

Observations of active galactic nuclei (AGN) in all bands of the electromagnetic spectrum have been reviewed by Wiita (1985). He concentrated on quasars, radio galaxies, Seyfert galaxies and BL Lacertae objects, with an emphasis placed on the energy production efficiency, compactness and variability. Observations have revealed that many compact radio sources have, in addition to the usual long-term variability, an intrinsic variability with time-scales less than a day. Heeschen et al. (1987) found, quite unexpectedly, variations of ~1 d at a wavelength of 11 cm in several flat-spectrum sources. Observations of intraday radio variability in compact radio sources and their probable explanation are given by Quirrenbach (1990).

Generally, the time-scale of the amplitude variation is associated with the size of the emitting region, such that shorter time-scales are associated with smaller regions. (Time-scales refer to the e-folding time or the doubling time of the amplitude.) However, variations observed for durations shorter than, for example, the doubling time may not, when extrapolated to actual doubling time, provide a meaningful limit on the physical size of the emitting region.

Optical variations in blazars on time-scales ranging from a few minutes to decades are well established (e.g. Webb et al. 1988). In several instances, day-to-day changes of more than 1 mag have been observed to occur (Smith & Hoffleit 1963; Angione 1969; Shen & Usher 1970; Eachus & Liller 1975; Liller & Liller 1975; Miller 1975, 1977). For example, Oke (1967) observed a 0.25-mag change in 1 d for 3C 279; Bertaud et al. (1973) reported a variation for BL Lacertae of 1.3 mag in 1 d and of 0.7 mag in 74 min. Racine (1970) detected optical variability of 0.1 mag within a few hours in BL objects.

OJ 287 is the only AGN for which claims have been made (Kiplinger 1974; Folsom et al. 1976; Smith et al. 1985) for the existence of periodicity P less than 1 d. Visvanathan & Elliot (1973) reported the detection of $P = 39.2$ min in the optical band, which was later confirmed by Frolich (1973). Carrasco, Dultzin-Hacyan & Cruz-Gonzalez (1985) reported the existence of $P = 23.0$ and 40.0 min in OJ 287. This object's long history of variability, the evidence of variability with time-scales of 1 d or less and the possibility that such variability may be periodic conspire to make this object a prime candidate for the investigation of microvariability.

There are several mechanisms which can account for the radio variability and the spectral characteristics of AGN. Details of the time dependence and the polarization behaviour of the flux are needed to separate the intrinsic variability from the propagation effects.

One might expect that the rapid optical variability of blazars could be explained by gravitational microlensing. However, the comparatively large size of the nuclei of AGN in the radio regime (enforced by the Compton brightness limit) tends to smear out

such variations, unless the Einstein radii of the microlenses are large. Lensing by massive stars ($M \leq 100\ M_\odot$) could account for variations in the cm regime, but apparent transverse velocities of order $40c$, much higher than observed in superluminal sources, are required to produce time-scales of ~ 1 d. Moreover, the amplitude of the variations is expected to increase with frequency, since the source size scales roughly with λ^{-1}; this clear contradiction with the observed behaviour of quasar 0917 + 624 seems to rule out microlensing as a possible explanation for rapid variability (Quirrenbach 1990).

Another more plausible mechanism for intraday radio variability is refractive interstellar scintillation (RISS). The wavelength dependence and short time-scale of the variations, however, argue against this explanation; very small scatterers must be present close to the Sun (≤ 100 pc) if this is the mechanism. Heeschen et al. (1987) speculated that unusual filaments associated with the galactic loop III could be responsible for an enhanced scattering in high-declination sources, but the statistics of intraday variations in (Quirrenbach 1990) samples with $60° \leq \delta \leq 90°$ and $35° \leq \delta \leq 50°$ are consistent with each other, indicating that the observed effects do not depend on celestial coordinates. Polarization variations and possible correlations with optical variability present further difficulties for the RISS hypothesis. Intrinsic variability seems therefore to be the most plausible explanation for the intraday variability.

Effects such as the absorption, spectral modification and change in polarization of intense radiation propagating through plasma in AGN have been explained by a sequence of plasma processes and have been shown to be much faster than single-particle processes (e.g. Krishan & Wiita 1986, 1990; Krishan 1988; Beal 1990; Gangadhara & Krishan 1990). The stimulated Compton and Raman scatterings for the generation of continuum radiation from relativistic electron beams in the quasar have been shown to be efficient processes (Gangadhara & Krishan 1992). The generation of such beams has been explained in many accretion scenarios for AGN (e.g. Lovelace 1976; Blandford & Payne 1982; Wiita, Kapahi & Saikia 1982; Rees 1984).

The radio flux of pulsars fluctuates over time-scales of 1 μs to 1 yr. Observations of pulsars PSR 1133 + 16 at 600 MHz and PSR 1944 + 17 at 1.4 GHz, made by Cordes (1983), showed a pulse sequence, with a broad range of quasi-periodic and intermittent stuctures, which is weakly frequency-dependent. Intrapulse fluctuations, revealed most effectively by autocorrelation analysis of the intensity and/or Stokes parameters, include narrow spikes and micropulses with durations from 1 μs to a few ms which also show quasi-periodicities of 0.1 to a few ms. Broader features and subpulses ($\Delta t \approx 1$–100 ms) sometimes appear as envelopes of micropulses and as modulations of amorphous noise-like structures. From the central limit theorem, one concludes that a large number of independent emitters contribute to the signal in a resolution time of 1–10 μs, so even the narrow micropulses may be incoherent composites of many coherent emissions.

The observational data (Gil 1986; Smirnova et al. 1986; Smirnova 1988) strongly support the hypothesis that pulsar micropulses are a temporal phenomenon and can be interpreted within the amplitude-modulation mechanism (Rickett 1975). As discussed by Chain & Kennel (1983) and others (Mofiz, de Angelis & Forlani 1985), modulational instability provides a natural mechanism for amplitude modulation. According to pulsar models (Ruderman & Sutherland 1975; Arons & Scharlemann 1979), the pulsar magnetosphere is composed of secondary electrons and positrons.

In this paper, we consider the modulational instability of a large-amplitude, linearly polarized electromagnetic (EM) wave propagating in an electron–positron plasma. We take into account the combined effects of relativistic mass variation of plasma particles, harmonic generation, and the finite-frequency electrostatic density perturbations which are created by the ponderomotive force of the EM wave. We show that modulation instability is a possible mechanism for the short-time intrinsic variability of compact radio sources. In addition to accounting for the extremely short time variability, this mechanism could prove to be a valuable diagnostic for the source region. In contrast, other mechanisms, such as refractive interstellar scintillation and microlensing, depend on very specific conditions far away from the source of the radiation.

2 THE MODULATIONAL INSTABILITY

An electron–positron plasma is found in the early Universe (Rees 1983), in active galactic nuclei (AGN) (Miller & Wiita 1987), in pulsar atmospheres (Goldreich & Julian 1969) and in the Van Allen Belt (Voronov et al. 1986). The collective plasma effects in an electron–positron plasma are of significant interest (e.g. Lominadze, Machabelli & Usov 1983; Shukla et al. 1986). Lately, the processes of non-linear wave conversion (Gedalin, Lominadze & Stenflo 1985) and self-modulation of EM waves have attracted a great deal of attention (Chain & Kennel 1983; Shukla 1985; Mofiz, de Angelis & Forlani 1985; Kates & Kaup 1989; Tajima & Taniuti 1990).

In an AGN, the electron–positron plasma exists at a distance of about $r \geq 10 R_{Sh}$ from the central engine (Lightman 1983), where $R_{Sh} = 2GM/c^2$ is the Schwarzschild radius. In pulsars, the plasma exists at a distance of about $r \geq 100 R_{ns}$ from the neutron star (Cordes 1983), where $R_{ns} \sim 10$ km is the neutron-star radius. In the present model, the electron–positron plasma is considered to be uniform and at rest with respect to the source of radiation.

Let us consider the non-linear propagation of a large-amplitude, linearly polarized EM wave with an electric vector

$$\boldsymbol{E}_0 = E_0 \cos(\boldsymbol{k}_0 \cdot \boldsymbol{r} - \omega_0 t)\,\hat{\boldsymbol{e}}$$

through an electron–positron plasma. The EM wave can cause such non-linear effects as charged particle mass modulation, harmonic generation and forced density perturbations. The non-linear processes occur on a time-scale slower than the radiation

oscillation period and are responsible for the spatio-temporal modulation of the EM wave packet. The charged particle mass modulation arises from relativistic mass variation in the EM fields, whereas the harmonic generation is due to the coupling of the particle quiver velocity with the radiation magnetic field. On the other hand, radiation pressure creates forced density perturbations ($\boldsymbol{k}$, ω). Thus a constant-amplitude EM wave interacting with small-amplitude non-resonant perturbations will generate upper ($\boldsymbol{k}_0+\boldsymbol{k}$, $\omega_0+\omega$) and lower ($\boldsymbol{k}_0-\boldsymbol{k}$, $\omega_0-\omega$) EM sidebands. The non-linear processes, as described above, provide the possibility of coupling sidebands with the original pump. A low-frequency non-linear force will result, which, in turn, will reinforce the low-frequency perturbations, thereby lending support to the amplitude modulation of the radiation.

The non-linear interaction of a large-amplitude, plane-polarized EM wave with an electron–positron plasma is governed by

$$\frac{\partial \rho}{\partial t}+\nabla\cdot\boldsymbol{J}=0, \tag{1}$$

$$m_j\left(\frac{\partial}{\partial t}+\boldsymbol{v}_j\cdot\nabla\right)(\Gamma_j\boldsymbol{v}_j)=q_j\left(\boldsymbol{E}+\frac{1}{c}\boldsymbol{v}_j\times\boldsymbol{B}\right)-\frac{\gamma_j T_j}{n_j}\nabla n_j, \tag{2}$$

$$\nabla\cdot\boldsymbol{E}=4\pi\rho, \tag{3}$$

$$\nabla\times\boldsymbol{E}=-\frac{1}{c}\frac{\partial\boldsymbol{B}}{\partial t} \tag{4}$$

and

$$\nabla\times\boldsymbol{B}=\frac{4\pi}{c}\boldsymbol{J}+\frac{1}{c}\frac{\partial\boldsymbol{E}}{\partial t}, \tag{5}$$

where $\Gamma_j=(1-v_j^2/c^2)^{-1/2}$ is the Lorentz factor, c is the speed of light, γ_j, n_j, $\boldsymbol{v}_j$, T_j, m_j and q_j are, respectively, the adiabatic exponent, the number density, the fluid velocity, the temperature, the rest mass and the charge of particle species j (equals e for electrons and p for positrons). Here, $\rho=e(n_\mathrm{p}-n_\mathrm{e})$ and $\boldsymbol{J}=e(n_\mathrm{p}\boldsymbol{v}_\mathrm{p}-n_\mathrm{e}\boldsymbol{v}_\mathrm{e})$ are the charge and the current densities. Equations (1) and (2) are the charge conservation and relativistic momentum equations, respectively, equation (3) is Poisson's equation and equations (4) and (5) are Maxwell's equations. We take $m_\mathrm{e}=m_\mathrm{p}=m_0$, $q_\mathrm{e}=-q_\mathrm{p}=-e$, where e is the magnitude of the electron charge. The electric and magnetic fields are given by

$$\boldsymbol{E}=-\nabla\varphi-\frac{1}{c}\frac{\partial\boldsymbol{A}}{\partial t} \tag{6}$$

and

$$\boldsymbol{B}=\nabla\times\boldsymbol{A}, \tag{7}$$

where φ and $\boldsymbol{A}$ are the scalar and vector potentials, respectively.

Inserting equations (6) and (7) into equation (5) and choosing Coulomb gauge $\nabla\cdot\boldsymbol{A}=0$, we can rewrite equation (5) as

$$\left(\nabla^2-\frac{1}{c^2}\frac{\partial^2}{\partial t^2}\right)\boldsymbol{A}=-\frac{4\pi}{c}\boldsymbol{J}+\frac{1}{c}\frac{\partial}{\partial t}(\nabla\varphi). \tag{8}$$

We now separate $\boldsymbol{J}$ into a transverse component $\boldsymbol{J}_\mathrm{t}$ (associated with the EM wave) and a longitudinal component $\boldsymbol{J}_\mathrm{l}$ (associated with forced electrostatic perturbations). The longitudinal part of $\boldsymbol{J}$ can be related to $\boldsymbol{E}=-\nabla\varphi$ via equations (1) and (3). By eliminating ρ between equations (1) and (3), we obtain

$$\nabla^2\left(\frac{\partial\varphi}{\partial t}\right)=4\pi\nabla\cdot\boldsymbol{J}.$$

Since $\nabla\cdot\boldsymbol{J}_\mathrm{t}=0$, we obtain

$$\nabla\left(\frac{\partial\varphi}{\partial t}\right)=4\pi\boldsymbol{J}_\mathrm{l}. \tag{9}$$

Substitution of equation (9) into equation (8) yields

$$\left(c^2\nabla^2-\frac{\partial^2}{\partial t^2}\right)\boldsymbol{A}=-4\pi c\boldsymbol{J}_{\rm t}. \tag{10}$$

The total transverse current density is defined as

$$\boldsymbol{J}_{\rm t}=e(n_{\rm p}\boldsymbol{u}_{\rm p}-n_{\rm e}\boldsymbol{u}_{\rm e}), \tag{11}$$

where the total particle number density and the rapidly varying (quiver) velocity are expressed as $n_j=n_0+n_{j\rm h}+n_{j\rm s}$ and $\boldsymbol{u}_j=\boldsymbol{u}_{j1}+\boldsymbol{u}_{j2}$, respectively. Here, the equilibrium number density n_0 is much larger than the first-order density perturbations (namely $n_{j\rm h}$ and $n_{j\rm s}$, which arise due to the harmonic generation and the radiation pressure, respectively).

The first- and second-order velocity vectors are given by $\boldsymbol{u}_{j1}=-q_j\boldsymbol{A}/m_0c$ and $\boldsymbol{u}_{j2}\approx(1/2)\,\boldsymbol{u}_{j1}u_{j1}^2/c^2$, respectively. Note that $\boldsymbol{u}_{j2}$ is associated with the gamma factor and represents the effect of weak relativistic particle-mass variation in the radiation fields.

For linearly polarized EM waves, the Lorentz force $\boldsymbol{u}_{j1}\times\boldsymbol{B}$ gives rise to a term which oscillates at the second harmonic. The corresponding density perturbation is

$$n_{\rm eh}=n_{\rm ph}=-\frac{n_0a^2(\omega_0^2-\omega_{\rm p}^2)}{(4\omega_0^2-\omega_{\rm p}^2)} \tag{12}$$

(Shukla et al. 1986), where $a=eA/m_0c^2$, and $\omega_{\rm p}=(4\pi n_0e^2/m_0)^{1/2}$ is the plasma frequency.

The total plasma current density is thus given by

$$\boldsymbol{J}_{\rm t}=-\frac{e^2}{m_0c}\left(1-\frac{qa^2}{2}\right)(2n_0+n_{\rm es}+n_{\rm ps})\boldsymbol{A}, \tag{13}$$

where $q=(3/4)-(\omega_0^2-\omega_{\rm p}^2)/(4\omega_0^2-\omega_{\rm p}^2)$. We note that $q=1/2$ for $\omega_0^2\gg\omega_{\rm p}^2$.

It is instructive to point out that for circularly polarized EM waves the harmonic generation non-linearity is absent and $n_{\rm eh}$ and $n_{\rm ph}$ are identically zero. For this case, equation (13) also holds with $q=1$.

We now suppose that

$$\boldsymbol{A}(\boldsymbol{r},t)=\frac{1}{2}[\boldsymbol{A}_{\rm s}(\boldsymbol{r},t)\,{\rm e}^{i(\boldsymbol{k}_0\cdot\boldsymbol{r}-\omega_0t)}+\boldsymbol{A}_{\rm s}^*(\boldsymbol{r},t)\,{\rm e}^{-i(\boldsymbol{k}_0\cdot\boldsymbol{r}-\omega_0t)}], \tag{14}$$

where $\boldsymbol{A}_{\rm s}(\boldsymbol{r},t)$ is a slowly varying function of space and time, and $\boldsymbol{A}_{\rm s}^*(\boldsymbol{r},t)$ is its complex conjugate. Squaring equation (14) on both sides, we obtain $A^2=(1/2)\,\boldsymbol{A}_{\rm s}\cdot\boldsymbol{A}_{\rm s}^*$, where we have neglected the higher frequency terms $2\omega_0$ because they are non-resonant.

Substituting the expressions for $\boldsymbol{J}_{\rm t}$ and $\boldsymbol{A}(\boldsymbol{r},t)$ into equation (10) and equating the coefficients of ${\rm e}^{i(\boldsymbol{k}_0\cdot\boldsymbol{r}-\omega_0t)}$ and ${\rm e}^{-i(\boldsymbol{k}_0\cdot\boldsymbol{r}-\omega_0t)}$ on both sides, we obtain

$$\left\{c^2\nabla^2+i2c^2\boldsymbol{k}_0\cdot\nabla-c^2k_0^2-\frac{\partial^2}{\partial t^2}+i2\omega_0\frac{\partial}{\partial t}+\omega_0^2-2\omega_{\rm p}^2\left[1-\frac{q}{4}\frac{e^2(\boldsymbol{A}_{\rm s}\cdot\boldsymbol{A}_{\rm s}^*)}{m_0^2c^4}\right]\right\}\boldsymbol{A}_{\rm s}=\frac{4\pi e^2}{m_0}(n_{\rm es}+n_{\rm ps})\left[1-\frac{q}{4}\frac{e^2(\boldsymbol{A}_{\rm s}\cdot\boldsymbol{A}_{\rm s}^*)}{m_0^2c^4}\right]\boldsymbol{A}_{\rm s} \tag{15}$$

and

$$\left\{c^2\nabla^2-i2c^2\boldsymbol{k}_0\cdot\nabla-c^2k_0^2-\frac{\partial^2}{\partial t^2}-i2\omega_0\frac{\partial}{\partial t}+\omega_0^2-2\omega_{\rm p}^2\left[1-\frac{q}{4}\frac{e^2(\boldsymbol{A}_{\rm s}\cdot\boldsymbol{A}_{\rm s}^*)}{m_0^2c^4}\right]\right\}\boldsymbol{A}_{\rm s}^*=\frac{4\pi e^2}{m_0}(n_{\rm es}+n_{\rm ps})\left[1-\frac{q}{4}\frac{e^2(\boldsymbol{A}_{\rm s}\cdot\boldsymbol{A}_{\rm s}^*)}{m_0^2c^4}\right]\boldsymbol{A}_{\rm s}^*. \tag{16}$$

Using $\boldsymbol{A}_{\rm s}(\boldsymbol{r},t)=\boldsymbol{A}_0+\delta\boldsymbol{A}(\boldsymbol{r},t)$, and linearizing equations (15) and (16), we have

$$\left[c^2\nabla^2+i2c^2\boldsymbol{k}_0\cdot\nabla-\frac{\partial^2}{\partial t^2}+i2\omega_0\frac{\partial}{\partial t}+\omega_0^2-c^2k_0^2-2\omega_{\rm p}^2\left(1-\frac{\varepsilon^2}{4}\right)\right](\boldsymbol{A}_0+\delta\boldsymbol{A})$$

$$=-\frac{\omega_{\rm p}^2}{2}\frac{qe^2}{m_0^2c^4}(\delta\boldsymbol{A}\cdot\boldsymbol{A}_0^*+\boldsymbol{A}_0\cdot\delta\boldsymbol{A}^*)\boldsymbol{A}_0+\omega_{\rm p}^2\delta N\left(1-\frac{\varepsilon^2}{4}\right)\boldsymbol{A}_0 \tag{17}$$

$$\left[c^2\nabla^2-i2c^2\boldsymbol{k}_0\cdot\nabla-\frac{\partial^2}{\partial t^2}-i2\omega_0\frac{\partial}{\partial t}+\omega_0^2-c^2k_0^2-2\omega_{\rm p}^2\left(1-\frac{\varepsilon^2}{4}\right)\right](\boldsymbol{A}_0^*+\delta\boldsymbol{A}^*)$$

$$=-\frac{\omega_{\rm p}^2}{2}\frac{qe^2}{m_0^2c^4}(\delta\boldsymbol{A}\cdot\boldsymbol{A}_0^*+\boldsymbol{A}_0\cdot\delta\boldsymbol{A}^*)\boldsymbol{A}_0^*+\omega_{\rm p}^2\delta N\left(1-\frac{\varepsilon^2}{4}\right)\boldsymbol{A}_0^*, \tag{18}$$

where $\delta\boldsymbol{A}(\boldsymbol{r}, t)$ is the perturbation, $\varepsilon^2 = qe^2|A_0|^2/m_0^2c^4$ and $\delta N = (n_{es} + n_{ps})/n_0$.

The relation between ε^2 and the luminosity of radiation L is given by

$$\varepsilon^2 = \frac{qe^2|A_0|^2}{m_0^2c^4} = \frac{2qe^2}{m_0^2c^3}\,\frac{1}{\omega_0^2}\,\frac{L}{r^2} = 2.1\times10^4\,\frac{q}{\omega_0^2}\,\frac{L}{r^2}, \tag{19}$$

where r is the distance between the source of radiation and the plasma medium.

From the zeroth-order terms in equations (17) and (18), we have

$$\omega_0^2 = 2\omega_p^2\left(1-\frac{\varepsilon^2}{4}\right) + c^2k_0^2. \tag{20}$$

This is the dispersion relation for an intense EM wave $(\boldsymbol{k}_0, \omega_0)$ propagating in an electron–positron plasma. It shows that the plasma frequency of the electron–positron plasma gets depleted by a factor of $\varepsilon^2/4$.

From the first-order terms in equation (17) and (18), we now find

$$\left[c^2\nabla^2 + i2c^2\boldsymbol{k}_0\cdot\nabla - \frac{\partial^2}{\partial t^2} + i2\omega_0\frac{\partial}{\partial t} + \omega_0^2 - c^2k_0^2 - 2\omega_p^2\left(1-\frac{\varepsilon^2}{4}\right)\right]\delta\boldsymbol{A}$$

$$= -\frac{\omega_p^2}{2}\,\frac{qe^2}{m_0^2c^4}(\delta\boldsymbol{A}\cdot\boldsymbol{A}_0^* + \boldsymbol{A}_0\cdot\delta\boldsymbol{A}^*)\boldsymbol{A}_0 + \omega_p^2\delta N\left(1-\frac{\varepsilon^2}{4}\right)\boldsymbol{A}_0 \tag{21}$$

and

$$\left[c^2\nabla^2 - i2c^2\boldsymbol{k}_0\cdot\nabla - \frac{\partial^2}{\partial t^2} - i2\omega_0\frac{\partial}{\partial t} + \omega_0^2 - c^2k_0^2 - 2\omega_p^2\left(1-\frac{\varepsilon^2}{4}\right)\right]\delta\boldsymbol{A}^*$$

$$= -\frac{\omega_p^2}{2}\,\frac{qe^2}{m_0^2c^4}(\delta\boldsymbol{A}\cdot\boldsymbol{A}_0^* + \boldsymbol{A}_0\cdot\delta\boldsymbol{A}^*)\boldsymbol{A}_0^* + \omega_p^2\delta N\left(1-\frac{\varepsilon^2}{4}\right)\boldsymbol{A}_0^*, \tag{22}$$

where $\omega_0 \gg \omega$ and ω is the frequency of the plasma slow motion. Fourier transformation of equations (21) and (22) with

$$\delta\tilde{\boldsymbol{A}}(\boldsymbol{k}, \omega) = \frac{1}{2\pi}\int_{-\infty}^{\infty}\int_{-\infty}^{\infty}\delta\boldsymbol{A}(\boldsymbol{r}, t)\,e^{-i(\boldsymbol{k}\cdot\boldsymbol{r}-\omega t)}\,d^3r\,dt \tag{23}$$

and

$$\delta\tilde{N}(\boldsymbol{k}, \omega) = \frac{1}{2\pi}\int_{-\infty}^{\infty}\int_{-\infty}^{\infty}\delta N(\boldsymbol{r}, t)\,e^{-i(\boldsymbol{k}\cdot\boldsymbol{r}-\omega t)}\,d^3r\,dt \tag{24}$$

gives

$$D_+\,\delta\tilde{\boldsymbol{A}} = \frac{\omega_p^2}{2}\,\frac{qe^2}{m_0^2c^4}(\delta\tilde{\boldsymbol{A}}\cdot\boldsymbol{A}_0^* + \boldsymbol{A}_0\cdot\delta\tilde{\boldsymbol{A}}^*)\boldsymbol{A}_0 - \omega_p^2\delta\tilde{N}\left(1-\frac{\varepsilon^2}{4}\right)\boldsymbol{A}_0 \tag{25}$$

and

$$D_-\,\delta\tilde{\boldsymbol{A}}^* = \frac{\omega_p^2}{2}\,\frac{qe^2}{m_0^2c^4}(\delta\tilde{\boldsymbol{A}}\cdot\boldsymbol{A}_0^* + \boldsymbol{A}_0\cdot\delta\tilde{\boldsymbol{A}}^*)\boldsymbol{A}_0^* - \omega_p^2\delta\tilde{N}\left(1-\frac{\varepsilon^2}{4}\right)\boldsymbol{A}_0^*, \tag{26}$$

where $D_\pm = (\boldsymbol{k}_0 \pm \boldsymbol{k})^2c^2 - (\omega_0 \pm \omega)^2 + 2\omega_p^2(1-\varepsilon^2/4)$ are the dispersion relations for the Stokes mode $(\boldsymbol{k}_s, \omega_s)$ and the anti-Stokes mode $(\boldsymbol{k}_a, \omega_a)$ when the following resonant conditions are satisfied:

$$\omega_0 - \omega = \omega_s, \qquad \boldsymbol{k}_0 - \boldsymbol{k} = \boldsymbol{k}_s,$$
$$\omega_0 + \omega = \omega_a, \qquad \boldsymbol{k}_0 + \boldsymbol{k} = \boldsymbol{k}_a. \tag{27}$$

Combining equations (25) and (26), we obtain

$$\delta\tilde{\boldsymbol{A}}\cdot\boldsymbol{A}_0^* + \boldsymbol{A}_0\cdot\delta\tilde{\boldsymbol{A}}^* = \left[-\omega_p^2|A_0|^2\left(1-\frac{\varepsilon^2}{4}\right)\delta\tilde{N} + \frac{\omega_p^2}{2}\varepsilon^2(\delta\tilde{\boldsymbol{A}}\cdot\boldsymbol{A}_0^* + \boldsymbol{A}_0\cdot\delta\tilde{\boldsymbol{A}}^*)\right]\left(\frac{1}{D_-}+\frac{1}{D_+}\right). \tag{28}$$

We must now calculate the low-frequency electron and positron density fluctuations n_{es} and n_{ps} produced by the radiation (ponderomotive) force $\boldsymbol{F}_\omega = -\nabla\psi_\omega$, where ψ_ω is the ponderomotive potential, which corresponds physically to radiation pressure. The ponderomotive force depends quadratically on the amplitude and produces a slowly varying longitudinal field, which leads to slow longitudinal motion and modifies the density. The ponderomotive potential is given by

$$\psi_\omega = \frac{e^2}{2m_0c^2}\langle A^2\rangle_\omega = \frac{e^2}{m_0c^2}\langle \boldsymbol{A}_s\cdot\boldsymbol{A}_s^*\rangle_\omega, \tag{29}$$

where the angular bracket $\langle\ \rangle_\omega$ represents the ω frequency component of an average over the fast time-scale $\omega_0 \gg \omega$. In the presence of the ponderomotive force, the slow motion of the plasma is governed by the following linearized equations:

$$\frac{\partial n_{js}}{\partial t} + n_0\nabla\cdot\boldsymbol{v}_{js} = 0, \tag{30}$$

$$\frac{\partial \boldsymbol{v}_{js}}{\partial t} = -\frac{q_j}{m_0}\nabla\varphi - \frac{1}{2}\frac{e^2}{m_0^2c^2}\nabla(\delta\boldsymbol{A}\cdot\boldsymbol{A}_0^* + \boldsymbol{A}_0\cdot\delta\boldsymbol{A}^*) - \gamma_j v_{tj}^2\nabla\left(\frac{n_{js}}{n_0}\right) \tag{31}$$

and

$$\nabla^2\varphi = -4\pi\sum_{j=e,p} q_j n_{js}, \tag{32}$$

where φ is the scalar potential associated with electrostatic perturbations and $v_{tj} = (k_B T_j/m_j)^{1/2}$ is the thermal velocity of the particle species j, where k_B is the Boltzmann constant.

When the continuity and momentum equations for the electron fluid are combined with equation (32), we obtain

$$\left(\frac{\partial^2}{\partial t^2} - \gamma_e v_{te}^2\nabla^2 + \omega_p^2\right) n_{es} = \omega_p^2 n_{ps} + S, \tag{33}$$

where the source term is defined as $S = (n_0e^2/2m_0^2c^2)\nabla^2(\delta\boldsymbol{A}\cdot\boldsymbol{A}_0^* + \boldsymbol{A}_0\cdot\delta\boldsymbol{A}^*)$.

Similarly, for the positron fluid, we have

$$\left(\frac{\partial^2}{\partial t^2} - \gamma_p v_{tp}^2\nabla^2 + \omega_p^2\right) n_{ps} = \omega_p^2 n_{es} + S. \tag{34}$$

Fourier-transforming equations (33) and (34), we obtain

$$(\omega^2 - \gamma_e k^2 v_{te}^2 - \omega_p^2)\tilde{n}_{es} = -\omega_p^2\tilde{n}_{ps} + \tilde{S} \tag{35}$$

and

$$(\omega^2 - \gamma_p k^2 v_{tp}^2 - \omega_p^2)\tilde{n}_{ps} = -\omega_p^2\tilde{n}_{es} + \tilde{S}. \tag{36}$$

In the absence of the EM wave, we obtain from equations (35) and (36)

$$1 - \sum_{j=e,p}\frac{\omega_p^2}{(\omega^2 - \gamma_j k^2 v_{tj}^2)} = 0, \tag{37}$$

which is the dispersion relation for electrostatic plasma oscillations in a warm electron–positron plasma. By summing equations (35) and (36) and assuming $\gamma_e = \gamma_p = \gamma$ and $T_e = T_p = T$, we obtain

$$(\omega^2 - \gamma k^2 v_t^2)\delta\tilde{N} = \frac{e^2}{m_0^2c^2}k^2(\delta\tilde{\boldsymbol{A}}\cdot\boldsymbol{A}_0^* + \boldsymbol{A}_0\cdot\delta\tilde{\boldsymbol{A}}^*), \tag{38}$$

where $v_t = (k_B T/m_0)^{1/2}$.

Substituting the expression for $\delta\tilde{N}$ from equation (38) into equation (28), we obtain

$$\left[1-\frac{\omega_p^2}{2}\varepsilon^2\left(\frac{1}{D_-}+\frac{1}{D_+}\right)\right](\omega^2-\gamma k^2 v_t^2)=-\omega_p^2 k^2 c^2\frac{\varepsilon^2}{q}\left(1-\frac{\varepsilon^2}{4}\right)\left(\frac{1}{D_-}+\frac{1}{D_+}\right). \tag{39}$$

This is the dispersion relation for the modulational instability of an EM wave propagating in an electron–positron plasma. Note that equation (39) is general and can be applied to the circularly polarized radiation for which $q=1$.

Since $\omega \ll \omega_0$, we have $D_\pm \approx k^2c^2 \pm 2\boldsymbol{k}\cdot\boldsymbol{k}_0c^2 \mp 2\omega\omega_0$. For a cold plasma (i.e. $\omega^2 \gg \gamma_j k^2 v_{tj}^2$), equation (39) can be written as

$$(\omega-\boldsymbol{k}\cdot\boldsymbol{v}_g)^2=\frac{1}{2}\frac{k^2c^2}{\omega_0}\left\{\frac{1}{2}\frac{k^2c^2}{\omega_0}-\frac{1}{2}\frac{\omega_p^2\varepsilon^2}{\omega_0}\left[1-\frac{2}{q}\frac{k^2c^2}{\omega^2}\left(1-\frac{\varepsilon^2}{4}\right)\right]\right\}, \tag{40}$$

where the group velocity of the EM wave is denoted by $\boldsymbol{v}_g=\boldsymbol{k}_0c^2/\omega_0$. The last two terms on the right-hand side of (40) are the contribution of the radiation pressure driven finite-frequency density perturbations.

In a special case, for $k=\varepsilon\omega_p/c$, the solution to equation (40) is given by

$$\omega=\frac{1}{2}\boldsymbol{k}\cdot\boldsymbol{v}_g\pm\frac{1}{2}\sqrt{(\boldsymbol{k}\cdot\boldsymbol{v}_g)^2\pm 2k^2c^2\frac{\omega_p}{\omega_0}\varepsilon\left[\frac{2}{q}\left(1-\frac{\varepsilon^2}{4}\right)\right]^{1/2}}. \tag{41}$$

Equation (41) predicts an oscillatory instability for

$$\varepsilon\left[\frac{2}{q}\left(1-\frac{\varepsilon^2}{4}\right)\right]^{1/2}>\frac{\omega_0(\boldsymbol{k}\cdot\boldsymbol{v}_g)^2}{2\omega_p k^2c^2},$$

and a typical growth rate is found to be

$$\Gamma_m\approx\left(\frac{2\omega_p^3}{\omega_0}\right)^{1/2}\varepsilon^{3/2}\left[\frac{2}{q}\left(1-\frac{\varepsilon^2}{4}\right)\right]^{1/4}. \tag{42}$$

It follows that the growth rate of the modulational instability for the case $k=\varepsilon\omega_p/c$ is proportional to $\varepsilon^{3/2}[2(1-\varepsilon^2/4)/q]^{1/4}$, in contrast to the growth rate of the relativistic modulational instability (Chain & Kennel 1983), which is proportional to ε^2.

Since $\omega \ll \omega_0$, the ω^4 and ω^3 terms in (39) can be dropped, and for $\varepsilon/\beta \ll v_t \ll c$, $\Phi\approx 90°$, $v_g\approx c$, $k\ll k_0$ and $q\approx 1/2$ we have expressions for the quasi-period of the modulation,

$$P=\frac{2\pi}{\omega_r}=\frac{2\pi}{\omega_0\cos\Phi}\frac{1}{y}, \tag{43}$$

and for the e-folding time,

$$t_e=\frac{1}{\Gamma}=\frac{6v_t}{\omega_0 c}\left(36\frac{v_t^2}{c^2}\cos^2\Phi-12\frac{\varepsilon^2}{\beta^2}\right)^{-1/2}\frac{1}{y}, \tag{44}$$

where $y=k/k_0$, $\beta=\omega_0/\omega_p$, Γ is the growth rate of the modulational instability, ω_r is the frequency of the electrostatic density perturbation and Φ is the angle between $\boldsymbol{k}_0$ and $\boldsymbol{k}$.

3 LARGE-AMPLITUDE EM WAVES IN AGN AND PULSARS AND THE EFFECT OF THEIR INCOHERENCE ON THE MODULATIONAL INSTABILITY

The above results have been derived assuming the incident field to be monochromatic. In reality, however, some amount of incoherence is always present. It has been shown by Tamour (1973) and Thomson et al. (1974) that the effect of the finite bandwidth $\Delta\omega_0$ of the incident field on the instability can be taken care of by replacing the damping rate of the sidebands Γ_L by $(\Gamma_L+2\xi)\approx(\Gamma_L+\Delta\omega_0)$, where ξ is the number of phase jumps per unit time. This replacement is possible because Γ_L is a measure of the length of time an electron is allowed to oscillate with the driving field before being knocked out of phase by a collision. The effective damping increases again when the driving field suffers a phase shift, and the two effects are additive. Thus replacement of Γ_L by $\Gamma_L+\Delta\omega_0$ certainly raises the threshold for the instability.

Another source of incoherence in the EM radiation is the lack of definite polarization. In an unpolarized beam, the tip of the electric-field vector undergoes random changes of direction. Thus an electron in such a field undergoes changes in its direction

of motion at the same rate. This essentially increases the effective collision frequency of the electrons and thus raises the threshold for the modulational instability. In the case of quasars, 1–10 per cent of the radiation is known to be polarized.

If Γ is the growth rate due to a monochromatic pump at ω_0, then the actual growth rate Γ' due to the broad pump with a spectral width $\Delta\omega_0 \gg \Gamma$ is given by

$$\Gamma' = \frac{1}{\Delta\omega_0}\Gamma^2 \tag{45}$$

(Kruer 1988).

Thus the reduction in the growth rate due to the finite bandwidth may be compensated to some extent by the high-luminosity radiation believed to be generated by coherent emission processes.

Several coherent processes, such as (i) emission from bunches of relativistic electron beams (Ruderman & Sutherland 1975), (ii) curvature radiation (Asséo, Pellat & Sol 1980; Gil & Snakowski 1990a,b) and (iii) the parallel acceleration mechanism (Melrose 1978), have been proposed for the radio emission from pulsars. On the other hand, the role of coherent emission processes in the generation of continuum emission from AGN was emphasized long ago (Burbidge & Burbidge 1967) and has now begun to receive the attention it deserves (Baker et al. 1988; Krishan & Wiita 1990; Weatherall & Benford 1991; Gangadhara & Krishan 1992; Lesch & Pohl 1992). Thus the presence of incoherence, due to finite bandwidth and lack of polarization in the radiation field, effectively increases the damping rate and therefore the threshold (in the kinetic treatment) and reduces the growth rate (t_e increases) of the modulational instability. Here, since we use a fluid treatment of the modulational instability, there is no damping of the sideband modes, and therefore there are no thresholds. However, due to a smaller pump luminosity being available (say 1–10 per cent) at a frequency ω_0, the growth rate Γ and frequency ω_r are reduced, with an attendant increase in the e-folding time t_e and the period P.

4 DISCUSSION

In this paper, we have shown that low-frequency electrostatic density perturbations can be non-linearly excited due to the interaction of a large-amplitude, linearly polarized EM wave with an electron–positron plasma. The superposition of low-frequency oscillations ($\boldsymbol{k}$, ω) over the high-frequency waves ($\boldsymbol{k}_0$, ω_0) produces an amplitude-modulated wave:

$$A(\boldsymbol{r}, t) = A_0\left[1 + \frac{\delta A}{A_0}\, e^{t/t_e}\cos(\boldsymbol{k}\cdot\boldsymbol{r} - t/P)\right]\cos(\boldsymbol{k}_0\cdot\boldsymbol{r} - \omega_0 t) \tag{46}$$

(from equation 14). Initially, δA is infinitesimally small, but it grows exponentially with time and reaches saturation due to some non-linear processes. Since the modulational instability has been investigated here in the linear regime, we can not find the depth of modulation. For the sake of illustration, with $\delta A/A_0 = 0.5$, $t_e = 200$ s and $P = 23$ min, we have plotted the amplitude-modulated vector potential as a function of time in Fig. 1. In the beginning, i.e. for $0 \le t \le 92$ min, δA is small and starts to grow exponentially. For $0 \le t < 92$ min, the incident radiation therefore remains unchanged; but for $t \ge 92$ min, δA grows and the radiation is modulated.

For the case of BL Lac object OJ 287, we derive a value of $\delta A/A_0 = 0.02$ from the observations of Carrasco, Dultzin-Hacyan & Cruz-Gonzalez (1985). For the plasma parameters assumed in Section 4.1 for an AGN, we obtain a period of 23 min. This

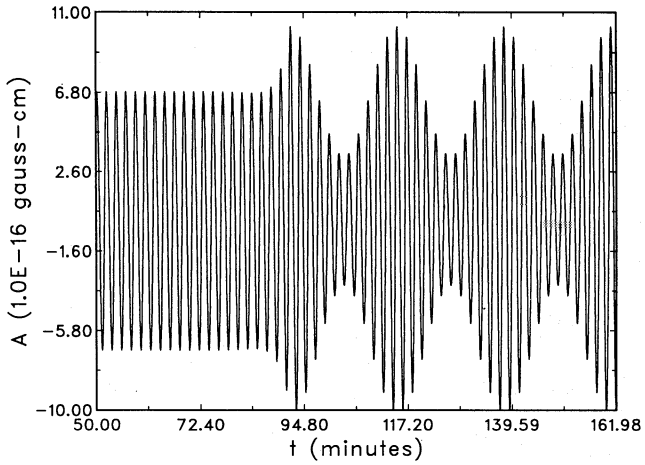

Figure 1. The modulated vector potential of the EM wave versus time t.

object has redshift $z=0.306$, magnitude $m_v=12$ and modulated luminosity $L=4\times10^{45}$ erg s^{-1}. Using $H_0=50$ km s^{-1} Mpc^{-1}, the value of A_0 corresponding to this luminosity is given by 6.86×10^{-16} G cm. For $t_e=200$ s, Fig. 2 shows the modulated flux $f=\omega_0^2|A(t)|^2/(8\pi c)$ as a function of time.

We solve equation (39) numerically, using conditions typical of an AGN and a pulsar, to find $\omega=\omega_r+i\Gamma=2\pi/P+i1/t_e$.

4.1 In an AGN

The typical values of the plasma and radiation parameters at a distance $r=r_{15}\times10^{15}$ cm from the central engine of an AGN are (Lightman & Zdziarski 1987; Krishan & Wiita 1990; Gangdhara & Krishan 1992) pair density $n_j=n_9\times10^9$ cm, temperature $T_j=T_4\times10^4$ K and luminosity in the radio band $L=L_{42}\times10^{42}$ erg s^{-1}. For $\Phi=90°$ the instability is growing only and non-periodic, but for $\Phi=0°$ the instability is purely oscillatory.

Fig. 3 shows the period $P=2\pi/\omega_r$ of the modulational instability of a radio wave of frequency $\nu_0=10^9$ Hz as a function of the wavenumber $y=k/k_0$ of the density perturbations at three plasma densities corresponding to $\beta=\omega_0/\omega_p=2$, 100 and 400. The figure shows that P is inversely proportional to y, as expected from equation (43). When $y\ll1$, P can be as large as a few days. The e-folding time t_e, i.e. the reciprocal of the growth rate of the modulational instability, is plotted as a function of y in Fig. 4. For $y\ll1$, t_e is inversely proportional to y, as expected from equation (44). (Note the logarithmic axes of these and following plots.)

Fig. 5 shows the period P as a function of L_{42}/r_{15}^2 for $\beta=2$, 100 and 400, and $y=10^{-9}$. This figure shows that the period P of the modulation is nearly independent of the value of L_{42}/r_{15}^2. The e-folding time t_e is plotted in Fig. 6 as a function of L_{42}/r_{15}^2. If we include the effect of incoherence in the incident radiation, then t_e will increase.

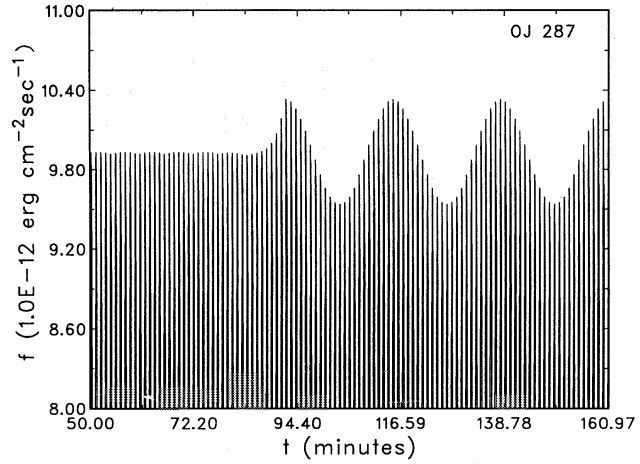

Figure 2. The theoretical light curve of BL Lac object OJ 287 showing the modulated emission of radiation.

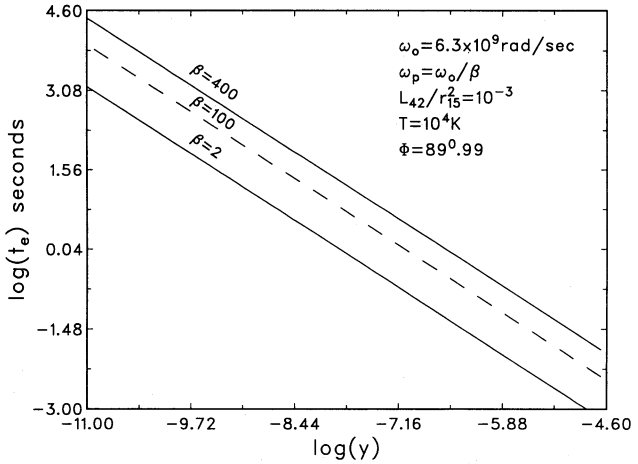

Figure 4. The e-folding time $t_e=1/\Gamma$ versus $y=k/k_0$ at three plasma frequencies, $\omega_p=\omega_0/2$, $\omega_0/100$ and $\omega_0/400$.

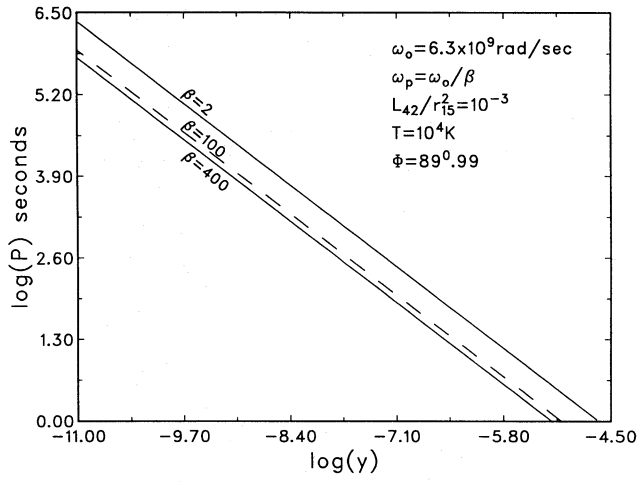

Figure 3. The period of modulation $P=2\pi/\omega_r$ versus the wavenumber $y=k/k_0$ of electrostatic density perturbations at three plasma frequencies, $\omega_p=\omega_0/2$, $\omega_0/100$ and $\omega_0/400$.

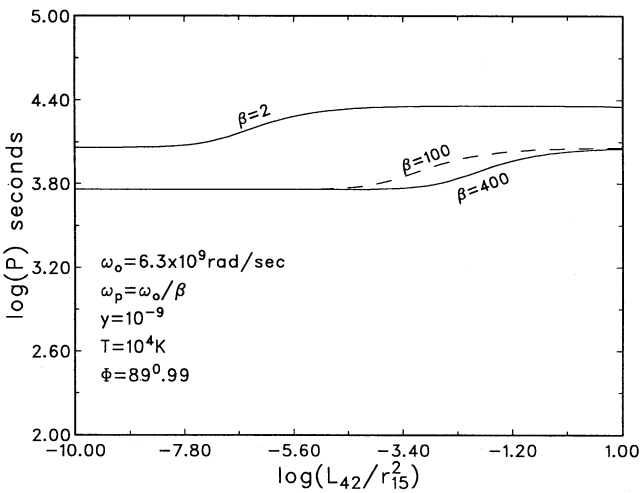

Figure 5. The period of modulation P versus L_{42}/r_{15}^2 at $\omega_p=\omega_0/2$, $\omega_0/100$ and $\omega_0/400$.

The period of modulation P is a strong function of the angle Φ (see Fig. 7). At frequencies close to the plasma frequency ($\omega_0 = 2\omega_p$), the instability occurs over a large range of Φ ($87.^{\circ}5 \leq \Phi \leq 92.^{\circ}5$). If the radiation frequency is much above the plasma frequency, then the instability is confined to a narrow range of Φ around 90°. The large-period ($P > 1$ h) pulses are produced when Φ is close to 90°.

Fig. 8 shows t_e as a function of Φ: when $\Phi \approx 90°$, t_e is small and the density perturbations grow very fast in time. The instability therefore becomes very strong near $\Phi \approx 90°$.

Figs 1–8 describe the modulational instability of a radio wave with frequency $\omega_0 = 6.3 \times 10^9$ rad s^{-1} for plasma parameters typical of an AGN. Consider now the modulation of optical radiation ($\omega_0 = 4 \times 10^{15}$ Hz) in the electron–positron plasma. The period $P = 2\pi/\omega_r$ versus $y = k/k_0$ is plotted in Fig. 9. For $\beta > 1000$, the period is independent of β. The value of the period of modulation P lies in the observed range of time-scales (10–50 min) of variations in the optical flux (Frolich 1973; Visvanathan & Elliot 1973; Kiplinger 1974; Folsom et al. 1976; Dultzin-Hacyan & Cruz-Gonzalez 1985; Smith et al. 1985). The figure shows that, at smaller wavenumbers $y < 10^{-10}$, pulses of $P > 1$ d are produced. Fig. 10 shows t_e as a function of y at three values of $\beta = 1000$, 2000 and 3000: t_e is inversely proportional to y for $y < 10^{-7.5}$. At $y = 10^{-7.5}$, growth rate is maximum. The modulational instability of X-ray radiation at $\beta \approx 10^5$ exhibits variations similar to those in the optical case.

The period of modulation P is independent of L_{42}/r_{15}^2 in the optical range (see Fig. 11). The values of $y = 5 \times 10^{-8}$, 2.5×10^{-8} and 1.7×10^{-8} adopted here are those values for which the growth rate is maximum in Fig. 10. At $y = 10^{-10}$, growth is not maximum but P is large. Fig. 12 shows t_e as a function of L_{42}/r_{15}^2, at different values of β and y.

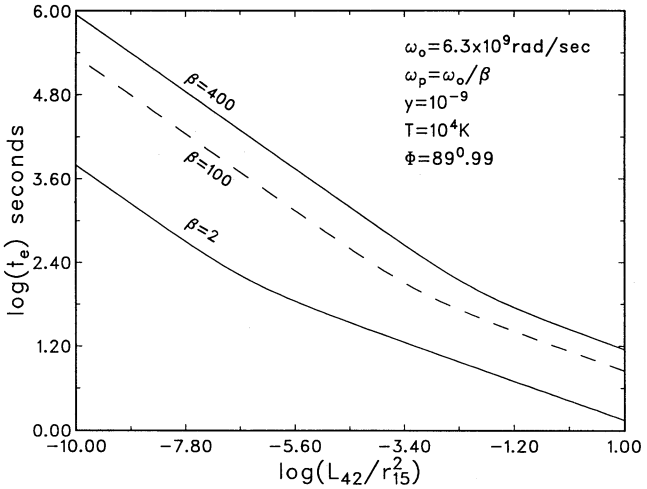

Figure 6. The e-folding time versus L_{42}/r_{15}^2 at $\omega_p = \omega_0/2$, $\omega_0/100$ and $\omega_0/400$.

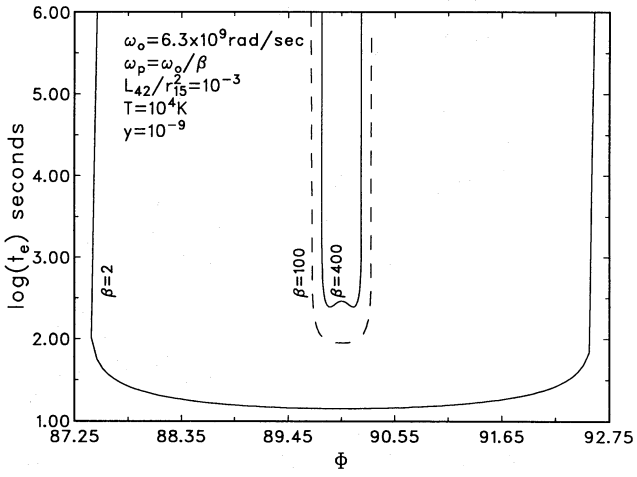

Figure 8. The e-folding time t_e versus $\Phi = \cos^{-1}(\hat{\boldsymbol{k}} \cdot \hat{\boldsymbol{k}}_0)$ at $\omega_p = \omega_0/2$, $\omega_0/100$ and $\omega_0/400$.

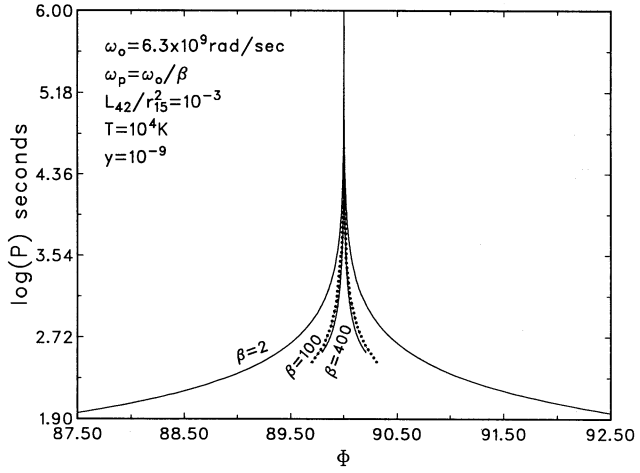

Figure 7. The period of modulation P versus $\Phi = \cos^{-1}(\hat{\boldsymbol{k}} \cdot \hat{\boldsymbol{k}}_0)$ at $\omega_p = \omega_0/2$, $\omega_0/100$ and $\omega_0/400$.

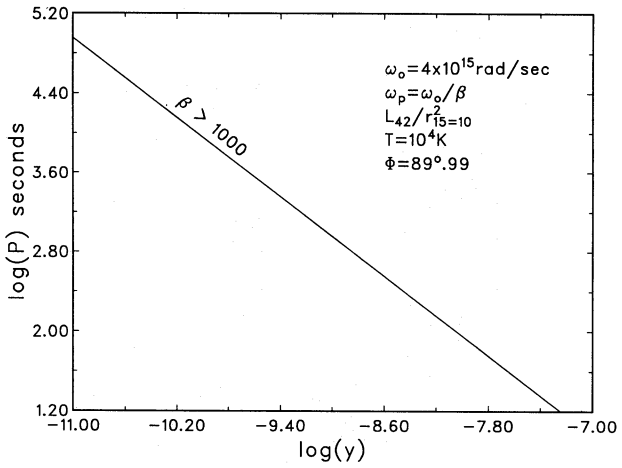

Figure 9. The period of modulation P of optical radiation versus y for $\beta > 1000$.

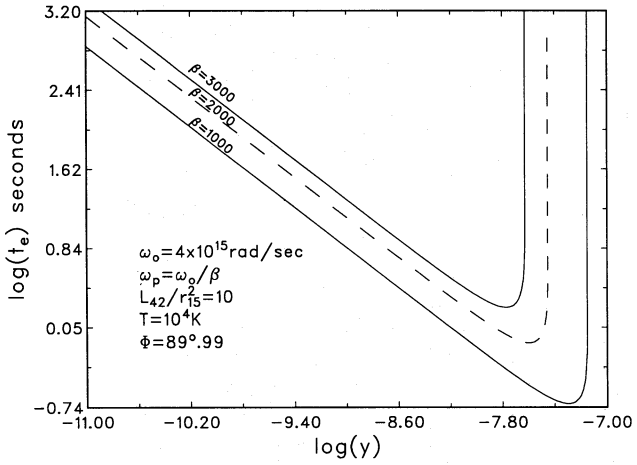

Figure 10. The e-folding time t_e versus y at $\beta = 1000$, 2000 and 3000.

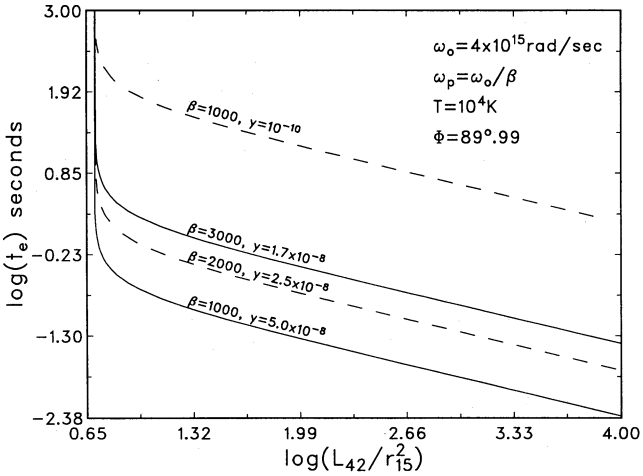

Figure 12. The e-folding time t_e versus L_{42}/r_{15}^2 at β and y as for Fig. 11.

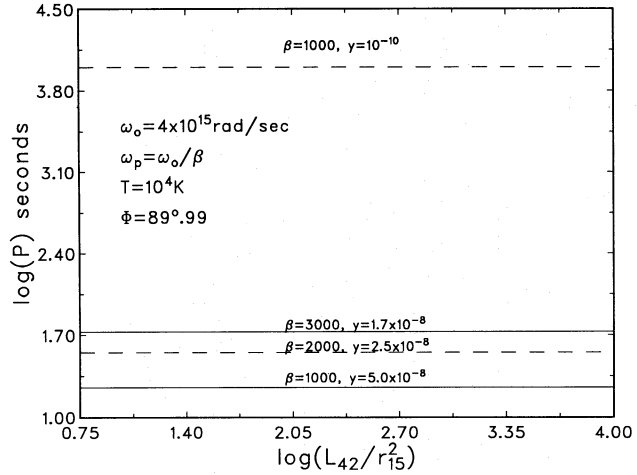

Figure 11. The period of modulation P of optical radiation versus L_{42}/r_{15}^2 at $\beta = 1000$, $y = 10^{-10}$; $\beta = 1000$, $y = 5.0 \times 10^{-8}$; $\beta = 2000$, $y = 2.5 \times 10^{-8}$ and $\beta = 3000$, $y = 1.7 \times 10^{-8}$.

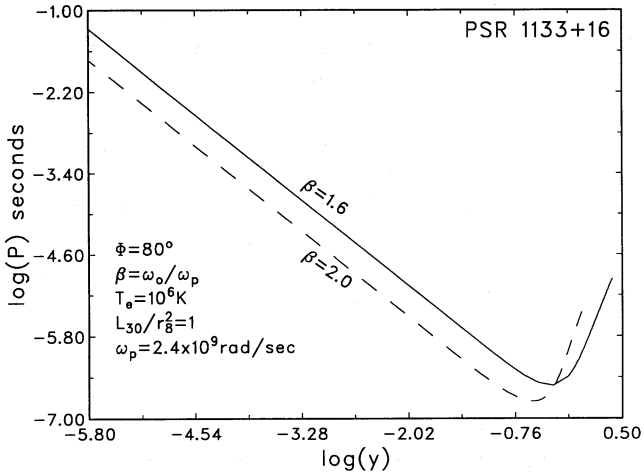

Figure 13. The period of modulation P versus y at $\beta = 1.6$ and 2 for PSR 1133 + 16.

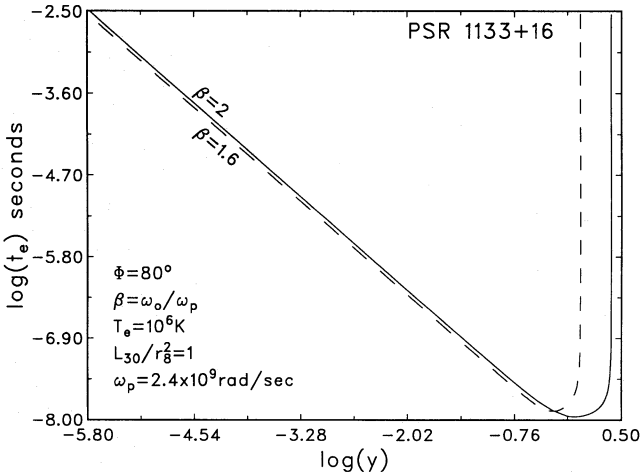

Figure 14. The e-folding time t_e versus y at $\beta = 1.6$ and 2 for PSR 1133 + 16.

4.2 In a pulsar

Typical values of the plasma and radiation parameters at a distance $r = 100R_{ns} = 10^8$ cm (neutron-star radius $R_{ns} \approx 10$ km) for the pulsar PSR 1133+16 are pair density $n_j = n_9 \times 10^9$ cm^{-3}, temperature $T_j = T_6 \times 10^6$ K and luminosity, in the band $\Delta\nu < \nu = 600$ MHz, $L = L_{30} \times 10^{30}$ erg s^{-1} (Cordes & Hankins 1977; Cordes 1983). Micropulses of duration 1 μs to a few ms at 600 MHz have been observed. Fig. 13 shows P as a function of y. The period P is found to lie in the observed range. Fig. 14 shows the e-folding time t_e as a function of y. The growth rate is a maximum at $y \approx 0.2$.

5 CONCLUSION

In our model, we have taken an electron–positron plasma with uniform and isotropic distributions of temperature and density. We have also assumed that the plasma is at rest with respect to the source of radiation. If the plasma is moving with relativistic velocities, then the relativistic effects must be taken into account. If the plasma is non-uniform in density and anisotropic in temperature ($T_e \neq T_p$), then $\nabla n_0 \neq 0$ and $\chi_e \neq \chi_p$. Tajima & Taniuti (1990) investigated the non-linear interaction of the EM wave and acoustic modes in an electron–positron plasma, invoking the assumption of quasi-neutrality in the dynamics of plasma slow motion and ignoring the relativistic mass variations of charged particles. Here we have investigated the non-linear interaction of the EM wave with electrostatic density fluctuations in an electron–positron plasma including harmonic generation and relativistic mass variation. The relativistic mass variation of electrons and positrons produces non-linear wave equations (15 and 16) for an EM wave propagating in the electron–positron plasma. The ponderomotive force of the EM wave leads to the excitation of low-frequency density perturbations. We have generalized the non-linear dispersion relation of Chain & Kennel (1983) to include the contribution of the forced electrostatic density fluctuations and the harmonic generation. The modulational instability of an EM wave produces localized EM pulses. This is an intrinsic process since it occurs in the source itself. The growth rate of the instability is proportional to $\varepsilon^{3/2}[2(1-\varepsilon^2/4)/q]^{1/4}$. The electron–positron plasma is modulationally unstable for either linear or circular polarization. A strong magnetic field can also affect the process: we intend to study this in detail in later work.

We believe that plasma processes such as modulational instability are potential mechanisms for the rapid variability and the production of micropulses in AGN and pulsars. Most of the mechanisms proposed previously require very specific environmental conditions; microlensing, for example, requires the nuclei of AGN to be large and transverse velocities to be of order $40c$, and refractive interstellar scintillation requires very small scatterers close to the Sun (≤ 100 pc) and unusual filaments associated with the galactic loop III. Since conditions for modulational instability exist naturally in the source region, modulation of the EM radiation may take place by this process.

ACKNOWLEDGMENTS

This paper was finalized when one of us (VK) was visiting Ruhr-Universität Bochum under the DLR/ISRO Exchange Programme. The support of DLR is gratefully acknowledged.

REFERENCES

Angione R., 1969, PASP, 80, 339
Arons J., Scharlemann E. T., 1979, ApJ, 231, 854
Asséo E., Pellat R., Sol H., 1980, in Sieber W., Wielebinski R., eds, Proc. IAU Symp. 95, Pulsars. Reidel, Dordrecht, p. 111
Baker D. N., Borovsky J. E., Benford G., Eilek J. A., 1988, ApJ, 326, 110
Beal J. H., 1990, in Brinkmann W., Fabian A. C., Giovannelli F., eds, Physical Processes in Hot Cosmic Plasmas. Kluwer, Dordrecht, p. 341
Bertaud Ch., Wlérick G., Véron P., Dumortier B., Bigay J., Paturel G., Duruy M., de Saevsky P., 1973, A&A, 24, 357
Blandford R. D., Payne P. G., 1982, MNRAS, 199, 883
Burbidge G. R., Burbidge E. M., 1967, Quasi-stellar objects. Freeman, San Francisco
Carrasco L., Dultzin-Hacyan D., Cruz-Gonzalez I., 1985, Nat, 314, 146
Chain A. C.-L., Kennel C. F., 1983, Ap&SS, 97, 9
Cordes J. M., 1983, in Burns M. L., Harding A. K., Ramaty R., eds, AIP Conf. 101 on Positron–Electron Pairs in Astrophysics. AIP, New York, p. 98
Cordes J. M., Hankins T. H., 1977, ApJ, 218, 484
Eachus A. D., Liller W., 1975, ApJ, 200, L61
Folsom G. H., Miller H. R., Wingert D. W., Williamon R. M., 1976, AJ, 81, 145
Frolich A., 1973, IAU Circ. 2525
Gangadhara R. T., Krishan V., 1990, JA&A, 11, 515
Gangadhara R. T., Krishan V., 1992, MNRAS, 256, 111
Gedalin M. E., Lominadze J. G., Stenflo L., 1985, Ap&SS, 108, 393
Gil J., 1986, ApJ, 308, 691
Gil J. A., Snakowski J. K., 1990a, A&A, 234, 237
Gil J. A., Snakowski J. K., 1990b, A&A, 234, 269
Goldreich P., Julian W. H., 1969, ApJ, 157, 869
Heeschen D. S., Krichbaum Th., Schalinski C. J., Witzel A., 1987, AJ, 94, 1493
Kates R. E., Kaup D. J., 1989, J. Plasma Phys., 42, 507
Kiplinger A. L., 1974, ApJ, 191, L109
Krishan V., 1988, MNRAS, 230, 183
Krishan V., Wiita P. J., 1986, in Swarup G., Kapahi V. K., eds, Proc. IAU Symp. 199, Quasars. Reidel, Dordrecht, p. 149
Krishan V., Wiita P. J., 1990, MNRAS, 246, 597
Kruer W. L., 1988, in Wylde A. M., ed., The Physics of Laser–Plasma Interactions. Addison-Wesley, New York, p. 70
Lesch H., Pohl M., 1992, A&A, 254, 29
Lightman A. P., 1983, in Burns M. L., Harding A. K., Ramaty R., eds, AIP Conf. 101 on Positron–Electron Pairs in Astrophysics. AIP, New York, p. 359

Lightman A. P., Zdziarski A. A., 1987, ApJ, 319, 643
Liller W., Liller M., 1975, ApJ, 199, L133
Lominadze J. G., Machabelli C. Z., Usov V. V., 1983, Ap&SS, 90, 19
Lovelace R. V. E., 1976, Nat, 262, 649
Melrose D. B., 1978, ApJ, 225, 557
Miller H. R., 1975, ApJ, 201, L109
Miller H. R., 1977, ApJ, 212, 153
Miller H. R., Wiita P. J., 1987, Active Galactic Nuclei. Springer-Verlag, Berlin
Mofiz U. A., de Angelis U., Forlani A., 1985, Phys. Rev. A, 31, 951
Oke J. B., 1967, ApJ, 147, 901
Quirrenbach A., 1990, in Miller H. R., Wiita P. J., eds, Meeting on Variability of Active Galactic Nuclei. Cambridge Univ. Press, Cambridge, p. 165
Racine R., 1970, ApJ, 159, L99
Rees M. J., 1983, in Gibbons G. W., Hawking S. W., Siklos S., eds, The Very Early Universe. Cambridge Univ. Press, Cambridge
Rees M. J., 1984, in Kellermann R. F., Setti G., eds, Proc. IAU Symp. 110, VLBI and Compact Radio Sources. Reidel, Dordrecht, p. 207
Rickett B., 1975, ApJ, 197, 185
Ruderman M., Sutherland P., 1975, ApJ, 196, 51
Shen B. S. P., Usher P., 1970, Nat, 228, 1070
Shukla P. K., 1985, Ap&SS, 114, 381
Shukla P. K., Rao N. N., Yu M. Y., Tsintsadze N. L., 1986, Phys. Rep., 138, 1
Smirnova T. V., 1988, Sov. Astron. Lett., 14, 20
Smirnova T. V., Solasnov V. A., Popov M. V., Novikov A. Yu., 1986, SvA, 30, 51
Smith H. E., Hoffleit D., 1963, Nat, 198, 650
Smith P. S., Balonek T. J., Heckert P. A., Elston R., Schmidt G. D., 1985, AJ, 90, 1184
Tajima T., Taniuti T., 1990, Phys. Rev. A, 42, 3587
Tamour S., 1973, Phys. Fluids, 16, 1169
Thomson J. J., Kruer W. L., Bodner S. E., DeGroot J., 1974, Phys. Fluids, 17, 849
Visvanathan N., Elliot J. L., 1973, ApJ, 179, 721
Voronov S. A., Gal'per A. M., Kirilov-Ugryumov V. G., Koldashov S. V., Popov A. V., 1986, JETP Lett., 43, 307
Weatherall J. C., Benford G., 1991, ApJ, 378, 543
Webb J. R., Smith A. G., Leacock R. J., Fitzgibbons G. L., Gombola P. P., Shepard D. W., 1988, AJ, 95, 374
Wiita P. J., 1985, Phys. Rep., 123, 117
Wiita P. J., Kapahi V. K., Saika D. J., 1982, Bull. Astron. Soc. India, 10, 304